Science of Sintering, **50** (2018) 409-419

doi: https://doi.org/10.2298/SOS1804409F

UDK 661.183.8; 622.785; 676.017.2

Physical Properties of Sintered Alumina Doped with Different Oxides

Suzana Filipović[1*)], Nina Obradović[1], Smilja Marković[1], Antonije Đorđević[2,3], Igor Balać[4], Aleksandra Dapčević[5], Jelena Rogan[5], Vladimir Pavlović[1]

[1]Institute of Technical Sciences of the Serbian Academy of Sciences and Arts, Knez Mihailova 35/IV, 11000 Belgrade, Serbia

[2]School of Electrical Engineering, University of Belgrade, Bulevar kralja Aleksandra 73, 11000 Belgrade, Serbia

[3]Serbian Academy of Sciences and Arts, Knez Mihailova 35, 11000 Belgrade, Serbia

[4]Faculty of Mechanical Engineering, University of Belgrade, Kraljice Marije 16, 11000 Belgrade, Serbia

[5]Department of General and Inorganic Chemistry, Faculty of Technology and Metallurgy, University of Belgrade, Karnegijeva 4, 11120 Belgrade, Serbia

Abstract:

Corundum (α-alumina) is a suiTab. material for usage in various industry fields owing to its chemical stability, electrical and mechanical features. It is known that properties of ceramics could be modified by addition of different oxides, as well as by changing the consolidation parameters. In this respect, alumina was doped with 1 wt.% of Cr_2O_3, Mn_2O_3 and NiO, followed by 1 hour of mechanical activation in a high-energy planetary ball mill. A sensitive dilatometer was used for sintering of powder mixtures up to 1400 ^oC and recording the obtained dilatation. The final density varied between cca. 1.9 and 3.3 g/cm^3. Microstructural changes were detected by SEM measurements. Changes in electrical permittivity and loss tangent were associated with the preparation conditions (types of additives, duration of mechanical activation). For a given mixture, the sintering increases the relative permittivity and decreases losses, exhibiting the optimal values of 8.32 and 0.027, respectively, for the sample activated 60 minutes and sintered, with the addition of MnO_2. Mechanical measurements indicate significant differences in strength with the addition of different transition metal oxides. Samples with Mn and Ni, activated and sintered, with strength of 121 and 86 MPa, respectively, have a significantly higher tensile strength than the other tested samples, due to their more compact microstructures.

Keywords*: Mechanical activation; Densities; SEM; Sintering; Alumina.*

1. Introduction

Alumina (Al_2O_3) can exist in several metasTab. phases, which irreversibly transform into α-alumina when heated to $\geq 1000\ ^oC$. In nature, it may occur as gemstones, having different colors depending on the dopants [1]. The α-alumina phase possesses strong ionic bonds inducing its well-known characteristic, such as hardness and stiffness. This type of bound usually gives rise to obtaining materials with high resistivity and low dielectric

*) **Corresponding author:** suzana.filipovic@itn.sanu.ac.rs

permeability. Alumina has a lot of excellent properties, such as hardness, dielectric and thermal properties and appropriate refractoriness, which give this material the opportunity for a wide range of applications [2, 3]. Corundum (α-alumina) is probably one of the most exploited materials in ceramic industry due to its useful properties and low cost. Therefore, this material attracts the attention of researchers even after a few decades of usage. In recent years, the interest in the synthesis of nanocrystalline alumina for many different applications has been increased [4].

It is well known that even a small addition of oxide influences the densification, reducing the sintering temperature, suppressing or promoting the grain growth, modifying the microstructure and mechanical properties [5-7]. For example, a small amount of MgO, which has been the most commonly used dopant for modification of the microstructure and properties of alumina, increases the hardness and fracture toughness [8]. Besides, transition metal oxides have been considered as important materials for doping of alumina, because of their electronic, optical, photonic and catalytic properties [9, 10]. Chromium has been widely used dopant for alumina as well. Alumina and chromium can form a substitutional solid solution $(Al_{2-x}Cr_x)O_3$ $(0 \leq x \leq 2)$ over the entire range of composition. This solid solution has many applications, such as in jewelry production, metalworking industries and aircraft engines, due to its high refractoriness and chemical stability [11]. It is well known that these properties do not depend only on the Al_2O_3–Cr_2O_3 solubility, but also on the relative density, i.e., porosity, which is mainly the consequence of the particle size and phase composition of starting components, method of preparation and sintering conditions. This gives a wide range of opportunities for future investigation [12, 13]. Furthermore, different manganese oxides (MnO_2, MnO) were employed in order to accelerate the sintering process and grain growth of alumina, and it was established that Mn^{2+} shifts the temperature of reaction to lower values [14-17]. These investigations were mostly performed on α-alumina as the starting material. Although the starting material certainly strongly affects the final mechanical and electrical properties, significantly less data are available for other modifications of Al_2O_3.

Consolidation parameters strongly influence the properties of ceramics. Therefore, one of the commonly used processes for enhancement of the material reactivity and particle size reduction is the mechanical activation. During the treatment, there is a significant increase in the concentration of structural defects near surface layers. These defects are also accompanied by a reduction of potential barriers for the process of nucleation of a chemical reaction. Besides its long-time usage, the milling is still an attractive method that enables the formation of submicrometer and/or nanostructured materials with desirable properties [18].

Having in mind that the preparation conditions strongly affect the structure and properties of alumina, the influence of the synthesis parameters on the final properties was investigated in this paper. Different transition metal oxides (Mn_2O_3, Cr_2O_3 and NiO) were added into the starting alumina (which was a mix of α-, γ-, κ-modification). The mixtures were milled for 60 minutes and thus prepared powders were examined by a dilatometer in order to determine changes in the dilatation of samples with the temperature increase. Afterwards, samples were subjected to measurements of mechanical and electrical properties as well as to the analysis of microstructure changes.

2. Materials and Experimental Procedures

Al_2O_3, Mn_2O_3, Cr_2O_3 and NiO powders (all 99 % purity Sigma–Aldrich, p.a.) were used for the experiments. Alumina powder was mixed with 1 wt.% of various oxides. The first set of mixtures was milled for only 1 minute for homogenization, and the other sets were milled for 60 minutes in a high-energy planetary ball mill (Planetary Ball Mill Retsch PM 100) using denatured ethanol as the milling medium. The milling conditions were as follows: Y-stabilized ZrO_2 vials and balls; ball-to-powder weight ratio of 30:1; rotation speed of

400 rpm. After milling, powders were dried at 100 °C for 1 hour and sieved. The samples were denoted as AM–1, AM–60, AC–1, AC–60, AN–1 and AN–60 according to the activation time and the type of the added oxide.

Green bodies in the shape of cylinders were prepared by uniaxial pressing (CARVER 3851-0) at 98 MPa. The theoretical density (TD) of the mixtures was 3.70 gcm^{-3} and it was calculated using the following equation, according to the rule of mixing [19]:

$$\rho_{mixture} = \frac{m_{mixture}}{V_1 + V_2} , \quad (1)$$

where m is the mass of the mixture (20.00 g), and V_1 and V_2 are the volumes of component 1 – Al_2O_3, and component 2 – Mn_2O_3, Cr_2O_3 or NiO, respectively, calculated using the TD of the components. Sintering was performed in air, heating the mixtures from the room temperature (RT) to 1400 °C at a heating rate of 10 $^oCmin^{-1}$ and dwell time of 1 hour, in a sensitive dilatometer (SETSYS Evolution TMA, Setaram Instrumentation, Caluire, France). The densities were determined by precise measurements of mass, diameter and thickness of the sintered specimens. After the sintering process, the samples were denoted as AM–1–1400, AM–60–1400, AC–1–1400, AC–60–1400, AN–1–1400 and AN–60–1400, according to the applied sintering temperature. The morphology of the sintered samples was analyzed by the scanning electron microscopy (JEOL JSM-6390 LV). Prior to SEM measurements, the samples were crushed and covered with gold.

The phase composition of alumina powder doped with manganese oxide was identified based on XRD data obtained on a Philips PW-1050 diffractometer with Cu-Kα radiation and a step/time scan mode of 0.05 °/s in the 2θ range 10–80°.

The relative dielectric permittivity (dielectric constant) and the loss tangent of the sintered samples were measured using an Agilent E5061A network analyzer, in the frequency range between 10 and 500 MHz. The samples were placed in a coaxial test chamber. The reflection coefficient of the chamber was measured by the analyzer and the relative complex permittivity of the samples was extracted using an electrostatic model.

In this study, the strength of the prepared samples was determined by the Brazilian test. Since 1943, the Brazilian test is a simple testing method to obtain the tensile strength of brittle material such as concrete, rock and ceramic materials [20]. In this test, a relatively thin circular disc or cylinder is compressed diametrically till failure occurs. The typical loading configuration is shown in Fig. 1.

The compression induces tensile stresses normal to the vertical diameter, which are essentially constant over a region around the center of the specimen. The indirect tensile strength is typically calculated based on the assumption that failure occurs at the point of maximum tensile stress, i.e., at the center of the disc. The suggested formula for calculating the splitting tensile strength σ_t (MPa) based on the Brazilian test is (ASTM 2008; ISRM 1978):

$$\sigma = \frac{2P}{\pi Dt} = 0.636\frac{P}{Dt} , \quad (2)$$

where P_{max} is the load at failure (N), D is the diameter of the test specimen (mm) and t is the thickness of test specimen measured at the center (mm). It is obvious that the lower punch is kept fixed, while the upper one is moveable by applying the load. The load is slowly increased until the failure occurs. The applied force (P) and the displacement (δ) are recorded till the failure.

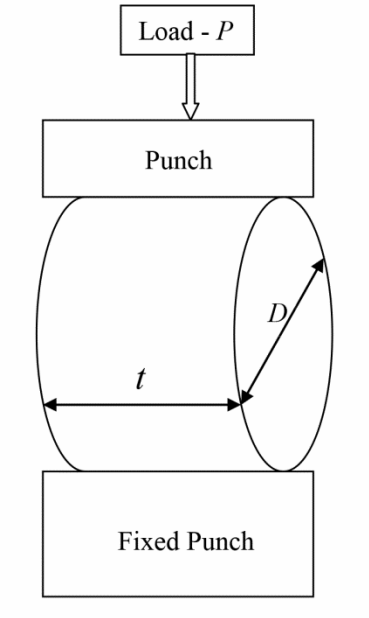

Fig. 1. Typical Brazilian test loading configurations in case of flat loading platens.

3. Results and Discussion

Fig. 2. shows the XRD pattern of the starting powder doped with manganese oxide, homogenized and mechanically activated for 60 minutes. Diffractograms of alumina doped with manganese oxide, AM–1, AM–60, are presented in order to confirm the presence of different phases of alumina and disordered structure. The starting alumina powder was a mix of a few phases (α-, κ-, γ-alumina, and $Al(OH)_3$), all identified by appropriate JCPDS cards (075-0783 for α-alumina, 052-0803 for κ-alumina, 079-1558 for γ-alumina, 072-0623 for $Al(OH)_3$). The broad and low-intensity peaks in diffractograms indicate that alumina was disordered. This is also the reason why the reflections belonging to highly crystallized Mn_2O_3 are clearly visible (JCPDS card 089-2809) although added in a small amount. The most pronounced peak of manganese oxide at 33 ° 2θ is sharp and intensive for both samples.

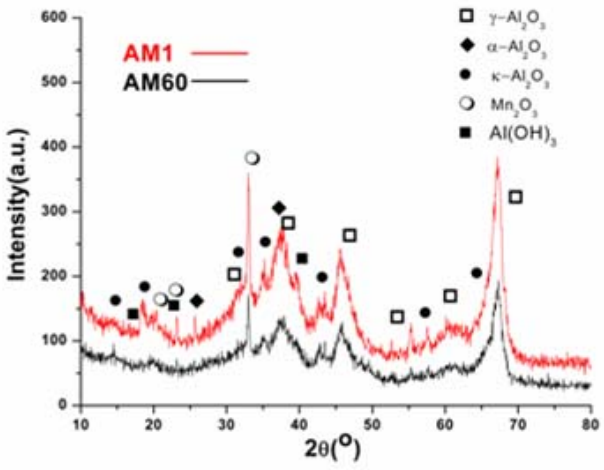

Fig. 2. XRD patterns of alumina doped with Mn_2O_3, homogenized and milled for 60 minutes.

Scanning electron micrographs of all sintered samples are presented in Fig. 3.

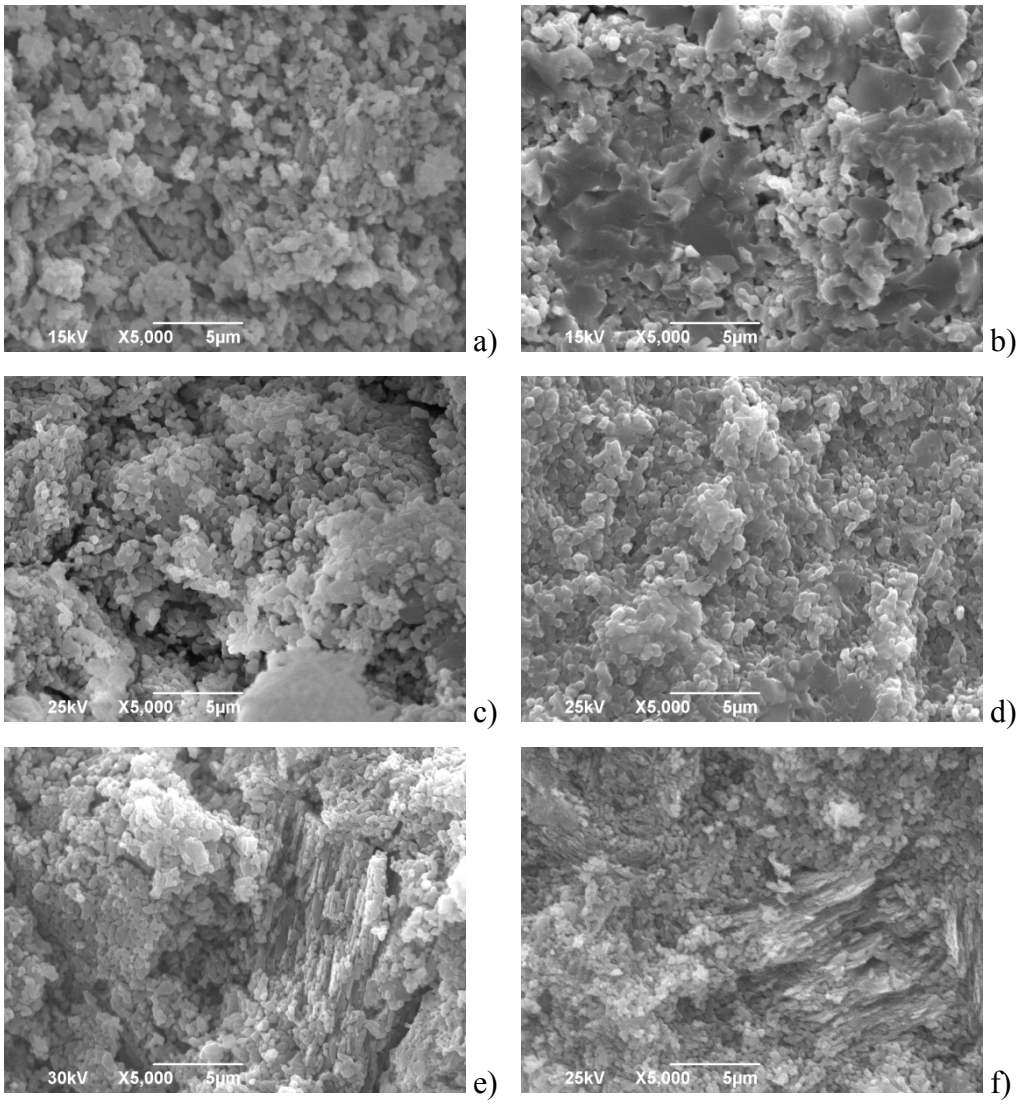

Fig. 3. SEM micrographs of sintered samples: a) AM–1–1400, b) AM–60–1400, c) AC–1–1400, d) AC–60–1400, e) AN–1–1400 and f) AN–60–1400.

Open porosity, small polygonally-shaped grains, 250–400 nm in size, as well as agglomerates, 2 microns in size, are observed in the sintered non-activated alumina sample with Mn_2O_3. The activation for 60 minutes prior to sintering process led to a denser microstructure, with closed pores and parts of well sintered grains. Plastered round grains that are less than 500 nm in size with agglomerates greater than 5 microns with open porosity are the main characteristics of the sample AC–1–1400. In Fig. 3d, closed packed spherical grains are observed. The particles retained their individuality. Contrary to that, the microstructures of sintered alumina samples doped with NiO show two different parts; the first one is similar to the previous ones (small round grains gathered to form agglomerates), but the other part represents an exception with elongated lamellas indicating liquid-phase sintering, where the liquid phase probably consisted of nickel according to the literature [21]. The formation of huge agglomerates was avoided due to the milling in a liquid medium [22].

Shrinkage curves for the non-activated and the activated sintered samples are presented in Fig. 4. The greatest shrinkage is observed for the activated alumina with NiO addition, while the smallest change in the sample thickness is noticed for the non-activated alumina with NiO addition. At the end of the heating regime, the sintering did not reach the

final stage, and the shrinkage was still taking place. As it can be seen in Fig. 4, the pallets expand on heating, and after reaching a maximum, they begin to shrink under the influence of the thermal profile. This could be related to an amorphous structure of the initial alumina. Such a behavior is often seen during sintering of amorphous systems and glasses, owing to the absence of long-range ordering [23, 24].

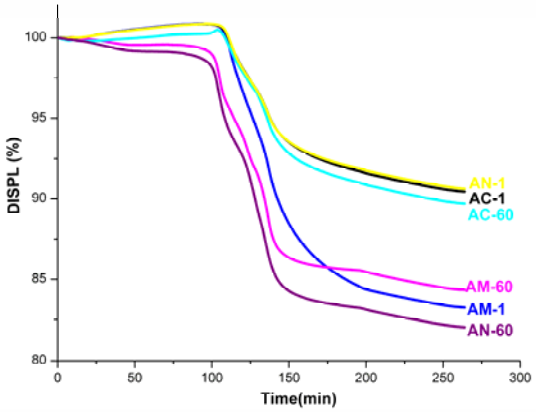

Fig. 4. Shrinkage of non-activated and activated alumina doped with different oxides during sintering at 1400 °C for 1 hour.

In order to achieve a better overview of the densification process and to determine characteristic temperatures, dilatometric curves are presented in Fig. 5.

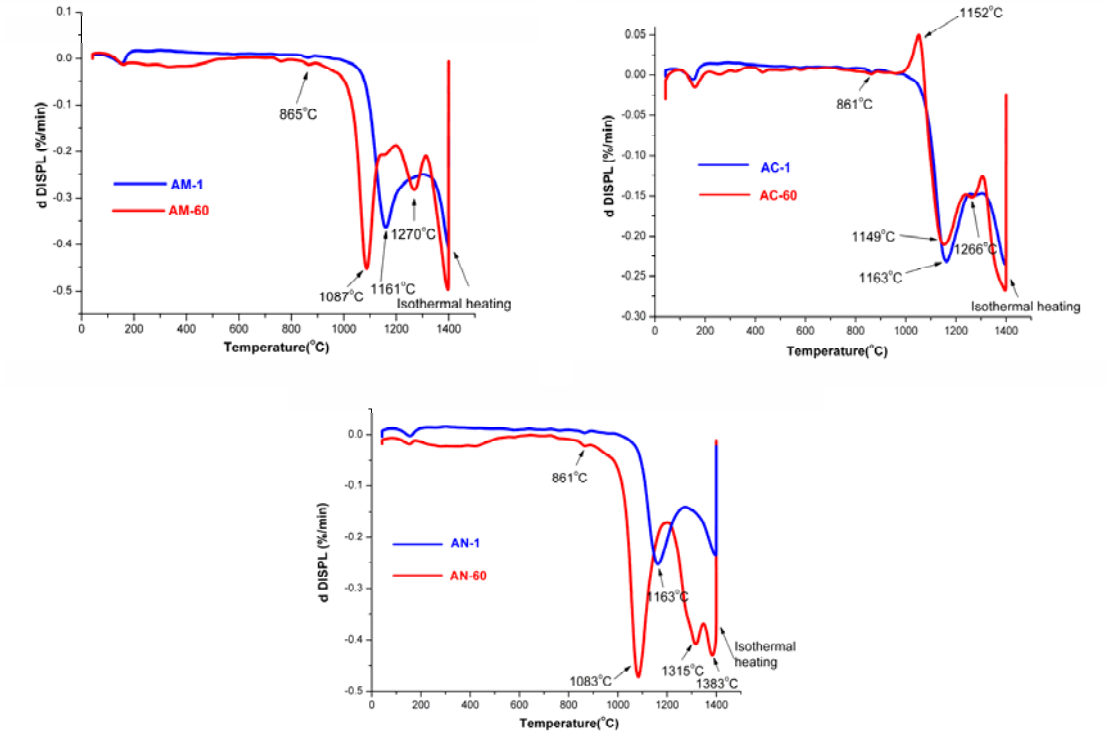

Fig. 5. Dilatometric curves of alumina doped with different oxides non-activated and activated for 60 minutes.

In all three Fig.s, the same temperature was observed (cca. 860 °C) corresponding to the alumina phase transformation γ → δ [25, 26]. The characteristic temperature for the next

phase transition, i.e., δ-alumina into the most stabile phase α-alumina [27], of about 1161 ^{o}C, was found for all non-activated samples. In all activated samples, that peak is shifted towards lower temperatures for almost 100 ^{o}C, indicating the presence of fragmented particles with a greater specific surface area and capable for reaction at lower temperatures than particles that were not activated [28]. Furthermore, the crystallization process detected at around 1270 ^{o}C in the activated samples (AM–60, AC–60, AN–60) is not present in the non-activated samples (probably because it is out of range, happening at > 1400 ^{o}C). Further, no great differences in temperatures of the phase transitions of alumina among AM–60, AC–60 and AN–60 samples were observed, probably due to similar microstructures as well as a small amount of added oxides. For the activated samples, the peak corresponding to sintering was detected slightly below 1400 ^{o}C, while this peak did not occur for AM–1, AC–1 and AN–1 samples due to the low final temperature used in the experiment. Besides the alumina phase transformations and crystallization, two peaks occurred at 1315 ^{o}C and 1383 ^{o}C for the sample AN–60, which correspond to the sintering of the sample (Fig. 4c). This could be a consequence of hard agglomerates presented in the activated AC-60 sample, which was also previously reported [29].

Geometrical and physical properties of prepared samples are presented in Tab. I. Relative densities, shrinkage and dielectric parameters are presented in Tab. II. The densities of all samples after sintering are in the range 1.93–3.30 g/cm^3, as presented in Tab. I. The lowest density, representing 52 % TD, is achieved for the AC–0–1400 sample, displaying the minimum shrinkage rate, less than 10 %. With activation prior to sintering, an increasing trend in the density is noticed, reaching the maximum, 89 % TD, for the AN–60–1400 sample, displaying the greatest shrinkage rate, almost 20 %.

Tab. I Dimensions and absolute densities of prepared samples.

Sample	**Density g/cm^3**	**D (mm)**	***t* (mm)**
AM–1–1400	2.55	6.725	2.715
AM–60–1400	2.81	6.434	2.428
AC–1–1400	1.93	7.466	2.745
AC–60–1400	2.88	6.780	2.280
AN–1–1400	2.10	7.140	2.725
AN–60–1400	3.30	6.570	1.980

The temperature of 1400 ^{o}C with the 1 hour dwell time was not sufficient to obtain higher densities, > 90 % TD, probably due to the low pressure during compaction (only 98 MPa). This is in accordance with SEM results and dilatometric measurements, which showed that no sample reached the final sintering stage, which lead to lower relative densities.

The dielectric permittivity of pure alumina is 9.3–11.5 [30]. We supposed that the addition of transition metal oxides in small amounts would decrease the permittivity. The obtained dielectric permittivity for all samples is in the range from 3.86 (for AC–0–1400) to 8.32 (for AM–60–1400). In general, the additives lowered the dielectric constant, while the mechanical activation increased it, but the permittivity is still below 10. The loss tangent is below 0.1, except for AC–0–1400 where it is 0.116, which could be correlated with the lowest density and shrinkage rate [31].

Tab. II Relative densities, shrinkage rates and dielectric parameters of sintered alumina with various additives (at 200 MHz).

Sample	Relative Density (% TD)	DISPL (%)	Relative permittivity	Loss tangent
AM–0–1400	68.92	83.20	5.10	0.048
AM–60–1400	75.95	84.30	8.32	0.027
AC–0–1400	52.16	90.40	3.86	0.116
AC–60–1400	77.84	89.70	5.24	0.050
AN–0–1400	56.76	90.60	3.90	0.081
AN–60–1400	89.19	82.10	7.63	0.066

As it is well known, the microstructure has a significant impact on mechanical properties. Less porosity in the material microstructure leads to higher material stiffness and strength, while an irregular shape of pores strongly influences the material fracture toughness and strength. As previously mentioned, the tensile strength of prepared samples was determined by Equation (2) after performing the Brazilian test. The obtained results for tensile strength, load at failure and displacement at failure for the tested specimens are presented in Tab. III.

Regarding the strength of the tested specimens, it can be concluded that samples marked as AM–60–1400 and AN–60–1400 with strength of 121 and 86 MPa, respectively, have a significantly higher tensile strength than the other tested samples, due to their more compact microstructures. It is evident that all samples exhibit better strength performance after the activation time of 60 minutes, which could be due to higher densities within the activated samples. Further, the SEM micrographs of the previously activated sintered samples indicate the beginning of the final sintering stage, which is correlated to a more solid structure. Also, the presence of the liquid phase occurred during the sintering of AN–60 promotes the strengthening of grains and also favorites the mass transport, leading to a decrease of the volume of pores.

Tab. III Tensile strength, load at failure, and displacement at failure.

Sample	P_{max} (N)	δ_{max} (mm)	σ_t (MPa)
AM–1–1400	506.86	0.114805	17.656
AM–60–1400	2938.15	0.257577	121.335
AC–1–1400	365.76	0.147919	11.351
AC–60–1400	600.48	0.149276	24.705
AN–1–1400	458.34	0.141819	14.982
AN–60–1400	1759.7	0.195479	86.033

4. Conclusion

Various oxides (Mn_2O_3, Cr_2O_3, NiO) were added to alumina powder. The first set of powders was obtained after a simple mixing for 1 minute, while the second set of samples

was activated in a planetary ball mill for 60 minutes. All mixtures were sintered at 1400 ^{o}C for 1 h in a dilatometer. The reduction of crystallization and the decrease in sintering temperatures of about 100 ^{o}C for the activated samples was observed. According to SEM images, the medium sintering stage occurs for the activated samples, while the initial sintering stage is a characteristic of non-activated samples. According to the measured strength, the activated and sintered alumina with the addition of NiO and Mn_2O_3 exhibits a relatively high resistance to the failure when loaded. The activation caused increased densities, tensile strength and dielectric permittivity, as well as decreased loss tangents.

Although the addition of different transition metal oxides showed a minor effect on the results of the dilatometric measurements, it influenced the physical properties of the prepared ceramics. On the other hand, the mechanical activation had a dominant effect on lowering the temperatures of phase transitions, crystallization and sintering.

The most favorable combinations of dielectric and mechanical properties were obtained for the activated and sintered alumina with the addition of NiO and alumina with the addition of Mn_2O_3, making them suiTab. candidates for potential applications in the production of smart jewelry.

Acknowledgments

This investigation was supported by the Serbian Ministry of Education, Science and Technological Development of the Republic of Serbia, and it was conducted under the following projects: OI 172057, III 45007 and III 45019.

5. References

1. C. Piconi, S. G. Condo, T. Kosmac, Alumina- and Zirconia-based Ceramics for Load-bearing Applications In book: Advanced ceramics for dentistry, Edition: 1st, Publisher: Butterworth-Heinemann, Oxford, Editors: Shen James, Chapter: 11, 2013.
2. I. S. A. Farag, I. K. Barrisha, M. M. Ei-Rafaay, Study of dielectric properties of α-alumina doped with MnO, CdO and MoO, Indian J. of Pure & App. Phys. 43 (2005) 446-458.
3. A. G. Tarasov, V. A. Gorshkov, V. I. Yukhvid, Phase composition and microstructure of Al_2O_3–Cr_2O_3 solid solutions prepared by self- propagating high-temperature synthesis, Inorganic Mater. 43 (2007) 724-728.
4. M. I. B. Bernardi, S. C. L. Crispim, A. P. Maciel ,A. G. Souza , M. M. Conceição , E. R. Leite, E. Longo, Synthesis and Characterization of Al_2O_3/Cr_2O_3-based Ceramic Pigments, J. Thermal Anal. and Calor. 75 (2004) 475-480.
5. H. Erkalfa, Z. Mm-h &T. Baykara, The Effect of $Ti0_2$ and $Mn0_2$ on Densification and Microstructural Development of Alumina, Ceram. Inter. 24 (1998) 81-90.
6. C. Wanga, Z. Zhao, Transparent polycrystalline ruby ceramic by spark plasma sintering, Mater. Res. Bull. 45 (2010) 1127-1131.
7. W. M. Shaheen, K. S. Hong, Thermal Characterization and Physicochemical Properties of Fe_2O_3.Mn_2O_3/Al_2O_3 Systems, J. Thermal Anal. and Calor. 68 (2002) 289-306.
8. D. Chakravarty, S. Bysakh, K. Muraleedharan, T.N. Rao, R. Sundaresan, J. Am. Ceram. Soc. 91 (2008) 203-208.
9. S. A. B. Asif, S. B. Khan, A. M Asiri, Visible light functioning photocatalyst based on Al_2O_3 doped Mn_3O_4 nanomaterial for the degradation of organic toxin, Nanoscale Res. Lett. 10 (2015) 355.

10. Valencia J, Arias NP, Giraldo O, Rosales-Rivera A. Synthesis and characterization of cobalt–manganese oxides. Phys B, 407(2012) 3155-7.
11. M. Nath, S. Sen, K. Banerjee, A.Ghosh, H.S.Tripathi, Densification behavior and properties of alumina–chrome ceramics: Effect of TiO_2, Ceram. Inter. 39 (2013) 227-232.
12. S. A. Cho, F. J. Arenas, J. Ochoa, Densification and hardness of Al_2O_3–Cr_2O_3 system with and without Ti addition, Ceram. Int. 16 (1990) 301-309.
13. K. Shibata, M. Yoshinaka, K. Hirota, O. Yamaguchi, Fabrication and mechanical properties of Cr_2O_3 solid solution ceramics in the system Cr_2O_3–Al_2O_3, Mater. Res. Bull. 32 (1997) 627-632.
14. D. Gouvea, R. L. Villalobos, J. D. T. Capocchi, Polymeric Precursor Synthesis of Alumina Containing Manganese Oxide Materials, Sci. For. 299–300 (1999) 91-98.
15. M. Ocaña, M. Martinez-Gallego, Preparation by hydrolysis of aerosols and properties of Cr, Mn and Co doped alumina spherical particles, Colloid Polym. Sci. 275 (1997) 1010-1017.
16. [16] R. H. R. Castro, D. Gouvea, Efeito do íon Mn como aditivo na transição de fase γ →α da alumina, Cerâmica, 49 (2003) 55–60.
17. M. Crisan, M. Rileanu, S. Preda, M. Zaharescu, A. M. Valean, E. J. Popovici, V.S. Teodorescu, V. Matejec, J. Mrazek, Manganese doped sol-gel materials with catalytic properties, J. Opto. and Adv. Mater. 8 (2006) 815-819.
18. S. Filipović, N. Obradović, V. B. Pavlović, M. Mitrić, A. Đorđević, M. Kachlik, K. Maca, Effect of consolidation parameters on structural, microstructural and electrical properties of magnesium titanate ceramics, Ceram. Int. 42 (2016) 9887-9898.
19. R. J. Magyar, S. Root, T. R. Mattsson, Equations of state for mixtures: results from density-functional (DFT) simulations compared to high accuracy validation experiments on Z, J. Phys.: Conference, 500 (2014) 162004.
20. T. Akazawa, New test method for evaluating internal stress due to compression of concrete: the splitting tension test. J Japan Soc Civil Eng, 29 (1943) 777-787.
21. M. Gizowska, A. Miazga , K. Konopka, M. Szafran, The influence of sintering temperature on properties of Al_2O_3-Ni composites, Compos. Theory Pract. 12 (2012) 33-38.
22. X. Kuang, X. Jing, Z.Tang, Dielectric Loss Spectrum of Ceramic $MgTiO_3$ Investigated by AC Impedance and Microwave Resonator Measurements, J. Am. Ceram. Soc. 89 (2006) 241-246.
23. T. K. S. Kumar, N. N. Viswanathan, H. M. Ahmed, C. Andersson, B. B. Rkman, Metall. Mater. Trans. B, 48 (2017) 746.
24. A. Karamanov, B. Dzhantov, M. Paganelli, D. Sighinolf, Glass transition temperature and activation energy of sintering by optical dilatometry, Thermo. Acta, 553 (2013) 1-7.
25. M. Bodaghi, A. R. Mirhabibi, H. Zolfonun, M. Tahriri, M. Karimi, Investigation of phase transition of γ-alumina to α-alumina via mechanical milling method, Phase Transitions, 81 (2008) 571-580.
26. B. Sathyaseelan, I. Baskaran, K. Sivakumar, Phase Transition Behavior of Nanocrystalline Al_2O_3 Powders, Soft Nanoscience Lett. 3 (2013) 69-74.
27. J. Lee, H. Jeon, D. G. Oh, J. Szanyi, J. H. Kwak, Morphology-dependent phase transformation of γ-Al_2O_3 Jaekyoung, App. Cataly. A: General, 500 (2015) 58-68.
28. N. Obradovic, N. Labus, T. Sreckovic, S. Stevanovic, Reaction Sintering of the 2ZnO-TiO_2 System, Sci. Sint. 39 (2007) 127-132.
29. Justyna Zygmuntowicz, Milena Piatek, Aleksandra Miazga, Katarzyna Konopka,Waldemar Kaszuwara, Dilatrometric sintering study and characterization of alumina-nickel composites, Process. and Appl. of Ceram. 12 (2018) 111-117.

30. Engineering ToolBox, (2010). *Relative Permittivity - the Dielectric Constant*. [online] Available at: https://www.engineeringtoolbox.com/relative-permittivity-d_1660.html.
31. Nina Obradović, Suzana Filipović, Nataša Đorđević, Darko Kosanović, Vladimir Pavlović, Dragan Olćan, Antonije Đorđević, Martin Kachlik, Karel Maca, Microstructural and Electrical Properties of Cordierite-based Ceramics Obtained After Two-step Sintering Technique, Sci. Sint. 48 (2016) 157-165.

Садржај: *Корунд (α-алумина) представља погодан материјал за примену у различитим гранама индустрије захваљујући хемијској стабилности, електричним и механичким својствима. Познато је да својства керамике могу бити модификована додатком различитих оксида као и мењањем параметара консолидације. У том светлу, алумина је допирана са 1 wt.% Cr_2O_3, Mn_2O_3 и NiO и механички активирана у високо-енергетском планетарном млину током 1 сата. Веома осетљив дилатометар је коришћен за синтеровање смеше прахова до 1400 ^oC и снимање примећене дилатације. Густине су варирале од 2-3.2 g/cm^3. Микроструктурне промене су детектоване помоћу скенирајућег електронског микроскопа. Промене електричне пермитивности и тангенса угла губитака су повезани са параметрима синтезе узорака (врсте адитива, трајања механичке активације). За дате смеше, синтеровање повећава пермитивност и смањује губитке, постижући оптималне вредности од 8,32 и 0,027, истим редом, за узорак активиран и синтерован, са додатком MnO_2. Мерења механичких својстава указују на значајне разлике у чврстоћи са додатком различитих оксида прелазних метала. Активирани и синтеровани узорци са додатком мангана и никла, са чврстоћом од 121 и 86 MPa, истим редом, имају значајно веће вредности затезне чврстоће од осталих испитиваних узорака, услед своје компактније микроструктуре.*
Кључне речи*: механичка активација, густине, SEM, синтеровање, алумина.*